

## **Coupling Effect on Propagation of Guided Waves in Engineering Structures and Human Bone Structures**

Jiangang Chen<sup>1)</sup>, \*Zhongqing Su<sup>2)</sup> and Li Cheng<sup>3)</sup>

<sup>1), 2), 3)</sup> *Department of Mechanical Engineering*  
*The Hong Kong Polytechnic University, Kowloon, Hong Kong*  
<sup>2)</sup> [mmsu@polyu.edu.hk](mailto:mmsu@polyu.edu.hk) (corresponding author)

### **ABSTRACT**

As a result of medium coupling, propagation characteristics of ultrasonic waves guided by a multi-medium system can be different from those in a homogeneous system. This phenomenon becomes prominent for a medium consisting of phases with considerably distinct material and physical properties (e.g., submerged structures or human bones covered with soft tissues). In the present study, the coupling effect arising from both fluid and soft tissues on wave propagation in engineering structures and human bone structures was explored and calibrated quantitatively, with a purpose of enhancing the precision of ultrasonic-wave-based non-destructive evaluation (NDE) and clinical quantitative ultrasound (QUS). Calibration results were used to rectify conventional NDE during evaluating corrosion in a submerged aluminum plate, and QUS during predicting the simulated healing status of a mimicked bone fracture. The results demonstrated that when the coupling effect was appropriately taken into consideration, the precision of NDE and QUS could be improved.

### **1. INTRODUCTION**

Propagation of elastic waves in the media comprising multiple phases is of a great interest in engineering practice. As a consequence of the medium coupling effect, elastic waves can be modulated, to different extents for different wave modes, presenting many somewhat subtle traits and behaving differently from their counterparts in a medium of a homogeneous nature. Most existing elastic-wave-based NDE techniques have been well-developed for materials or structures of a single component (e.g., homogeneous alloys) or multiple but similar components (composite laminates) in a free status. When applied to objects with coupled media (such as a boat hull, pillar of offshore platform or petroleum pipeline (solids) submerged in seawater

---

1) Research Associate, now postdoctoral research scientist in Department of Biomedical Engineering, Columbia University, NYC, The USA

2) 3) Professor

(fluid) (Na and Kundu 2002, chen *et al.* 2010)), the coupling effect can prevent these NDE techniques from delivering precise results. To calibrate and rectify the influence of medium coupling on wave propagation, in particular when the coupled medium has very distinct properties from the one principally accommodating wave propagation (*e.g.*, one being relatively 'soft' such as fluid or soft tissue, while the other relatively 'hard' such as alloy or cortical bone), remains relevant but challenging.

The coupling effect from fluid on elastic waves in plate/shell-like structures has been drawing attentions over the years (in these cases the elastic waves take the form of Lamb waves). Yapura and Kinra (1995) analytically studied the propagation of Lamb waves in a fluid-solid coupled bi-layer system, to show that the surrounding fluid could alter the properties of Lamb waves. This conclusion was experimentally validated by Moilanen *et al.* (2006). On the other hand, Lamb waves in thin-walled tubular structures were explored by Cheeke *et al.* (1999), to capture a decrease in the velocity when the tube was filled with fluid. All these studies have reached some important conclusions regarding the medium coupling effect on wave propagation, whereas hitherto there is a lack in quantitative compensation for such a coupling effect for practical implementation of ultrasonic-wave-based NDE.

The above concern also exists in medical ultrasound applications. In clinical quantitative ultrasound (QUS), apart from the degenerative disorders of bone, the coupled soft tissues (skin, muscle, marrow, *etc.*) can also modulate ultrasound waves propagating in bone (Moilanen *et al.* 2006). This effect is often ignored in clinical practice, and implementation of QUS is simply based on the simplified theorem of elastic waves in single-medium solids in a free status, leading to less precise assessment without differentiating the influence of coupled soft tissues from that due to the degradation in bone.

In this study, the coupling effect arising from fluid (in engineering aspect) and soft tissue mimicking (in biological aspect) on ultrasonic waves were investigated and calibrated quantitatively, via a three-dimensional (3D) finite element (FE) analysis and a testing approach. Calibration results were employed to rectify traditional NDE during detecting corrosion in a submerged aluminum plate and QUS during predicting the healing progress of mimicked bone fracture.

## 2. THEORY

In a medium comprising multi-phases (*e.g.*, a plate submerged in liquid or a pipe buried in soil, the human bone covered with a layer of soft tissue), the coupling between two phases introduces confinements to particulate motion at the interface, and provides a radiation way for Lamb waves in the plate to leak into the coupled medium, referred to as leaky Lamb waves. Under this coupling effect, Lamb waves in a multi-phase medium behave differently from those in a free plate, and moreover the influence can be distinct for different modes. In a preliminary estimate, considering a plate coupled with a fluid-like phase, energy associated with the fundamental

symmetric Lamb mode ( $S_0$ ) is mostly retained in the plate because fluid is unable to sustain shear (in-plane) loads and as a result it is difficult for in-plane particulate motion to cross the plate-liquid interface. In contrast, in a plate coupled with a medium supporting both the in-plane and out-of-plane particulate motion patterns (e.g., a composite laminate or a plate adhered with a layer of silicon rubber), partial energy of  $S_0$  mode can leak into the coupled medium through the interface. However, in both the above two cases, leakage of signal energy associated with the fundamental anti-symmetric Lamb mode ( $A_0$ ) is always anticipated. That is because in  $A_0$  mode the particles mostly have out-of-plane displacements and any coupled medium supports such a motion pattern. The above estimate will be investigated in this study.

In particular for an infinitely large fluid-solid coupled medium (fluid thickness:  $a$ , half plate thickness:  $h$ ), the characteristic equation for this two-phase medium can be described, if both the solid and fluid are deemed isotropic and the latter is unable to sustain shear loads, as (Moilanen *et al.* 2006)

$$\det(G(\omega, k, a, h, \rho, \rho_F, c_F, c_L, c_T)) = 0, \quad (1)$$

where  $G$  is the characteristic matrix,  $\omega$  the circular frequency,  $k$  the wavenumber,  $a$  and  $h$  the thickness of the coupled fluid layer and half thickness of the solid layer, respectively;  $\rho$  and  $\rho_F$  the density of the solid layer and coupled fluid layers, respectively;  $c_F$  the bulk wave velocity in the fluid layer;  $c_L$  and  $c_T$  the velocity of the longitudinal and transverse (shear) wave modes in the plate, respectively.

### 3. METHODOLOGY

Consider two scenarios: i) an aluminum plate ( $600 \times 600 \times 1.6 \text{ mm}^3$ ) coupled with a layer of water with the same in-plane dimension as that of the plate but different thicknesses (from 0 to 10 mm with an increment of 1 mm); and ii) a soft tissue-bone phantom that is comprised of a bone-mimic phase (using acrylic materials) ( $460 \times 240 \times 2 \text{ mm}^3$ ) and a soft tissue-mimic phase (using artificial silicon rubber (ASR)) with variance in thickness (i.e., 0.8, 1.9, 3.4, 4.2, 5.1, 6.3, 7.7, 9.4 mm). Two phases have the same in-plane dimensions and are tied through an interface. In what follows, both the aluminum and acrylic are called the *hard phase*, while water and ASR the *soft phase*.

#### 3.1. 3D FE Modelling and Simulation Technique

In FE modeling, the hard phase was modelled using 3D eight-node brick elements, while soft phase was modelled either using 3D eight-node acoustic elements (for water) or using 3D eight-node brick elements (for ASR). A pair of transmitter and receiver was placed in tandem at the interface of two phases (Fig. 1), to activate and receive ultrasonic waves in terms of axial transmission measurement. Note that, aimed at exploring the medium coupling effect on waves in bone, the transducer pair was positioned at the interface between two phases rather than atop the soft phase.

The interface between the hard and soft phases was modelled using a specialised surface-based coupling constraint in virtue of a node-to-surface formulation, which is provided by ABAQUS®/EXPLICIT and therein named 'TIE'. The transmitter and receiver were modelled using a piezoelectric model (Su and Ye 2009). Dynamic FE simulation was accomplished using commercial FE package ABAQUS®/EXPLICIT.

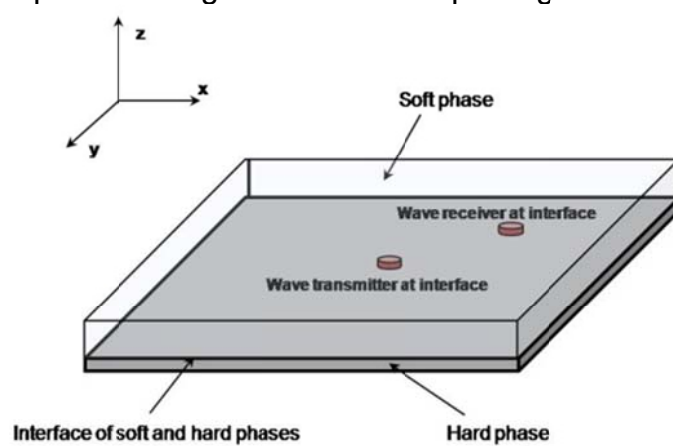


Fig. 1. Allocation of transmitter and receiver at the interface between soft and hard phases (in both 3D FE simulation and in vitro testing)

### 3.2. Testing Approach

An *in vitro* testing approach including supporting software/hardware for implementation was developed. A pair of water-proof ultrasound transducers (Panametrics-V303-SU, central frequency: 1 MHz, nominal diameter: 13 mm), serving as the wave transmitter and receiver, respectively, was instrumented with a signal generation and data acquisition system configured on a VXI platform (Su and Ye 2009), as shown in Fig. 2. The transducer pair was collocated at the interface of two phases, consistent with the above FE simulation. With the system, diagnostic signals, i.e., five-cycle *Hanning*-windowed sinusoid tonebursts, were first customised in MATLAB® and downloaded to an arbitrary waveform generation unit (Agilent® E1441), in which D/A conversion was performed. The analog signals were amplified to 180 V (peak-to-peak) with a linear amplifier (PiezoSys® EPA-104) to drive the transmitter. Wave signals were captured with the receiver through a signal digitiser (Agilent® E1438A) at a sampling rate of 25 MHz.

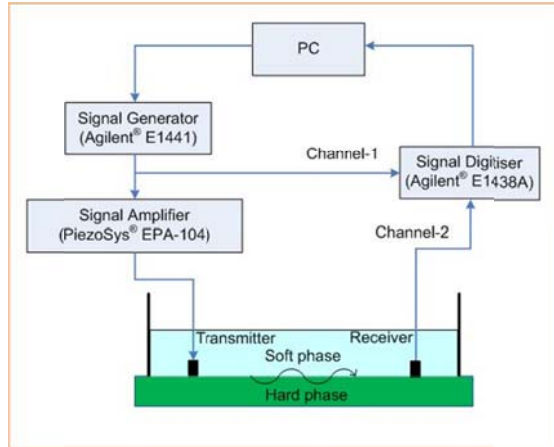


Fig. 2. Configuration of experimental setup for *in vitro* testing

## 4. RESULTS AND DISCUSSION

### 4.1. Coupling effect arising from fluid

The coupling effect arising from fluid was first investigated by ultrasonically interrogating an aluminium plate whose upper surface was in contact with a layer of pure water (the thickness of the water layer varied from 0 to 10 mm with an increment of 0.5 mm), via 3D FE modelling and simulation (Section 3.1) and experiment (Section 3.2).

Figure 3 shows velocities of two concerned wave modes, subject to thickness of the coupled soft phase, recapitulating that the coupled soft phase exerts strong influence on characteristics of the  $A_0$  mode. However it does not modulate  $S_0$  to a perceptible level. They also highlight that the most significant changes of  $A_0$  occur when the soft phase is initially introduced, and as thickness of the soft phase increases, further influence from soft phase is mild.

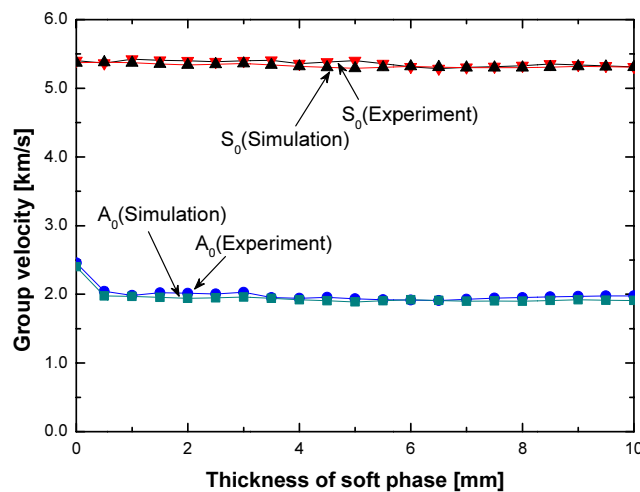


Fig. 3. Group velocities of  $S_0$  and  $A_0$  in an aluminium plate coupled with water layer of different thicknesses

Further, the above examination was extended to a sweep frequency range from 50 to 350 kHz. The dispersion curves of  $S_0$  and  $A_0$  in the aluminium plate in the absence and presence of fluid (thickness: 5 mm) were shown in Fig. 4. Based on the above results, influence of the fluid coupling on the propagation of the  $A_0$  mode was quantitatively calibrated, subjected to the thickness of the fluid layer.

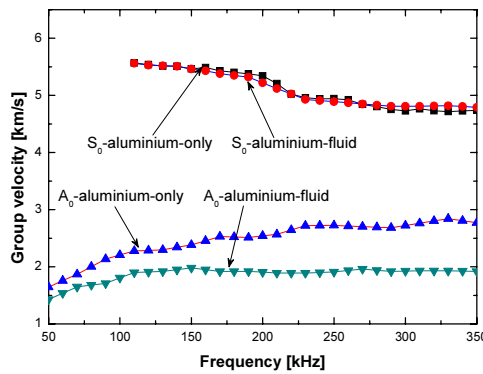


Fig. 4. Dispersion curves of Lamb waves in an aluminium plate in the absence and presence of a fluid layer (4 mm in thickness) obtained via FE simulation and experiment

#### 4.2. Coupling effect arising from soft tissue mimicking

The layers of ASR with different thicknesses (as mentioned in Section 3) but the same elastic properties ( $E_{ASR} = 11.96 \text{ kPa}$ ) were explored. Diagnostic signals, having the same waveform as the above case, were activated at a series of candidate frequencies ranging from 50 to 200 kHz, so as to ascertain the most optimal excitation frequency. Captured signals under excitation of 75 kHz showed the best recognisability for both  $S_0$  and  $A_0$ , and this frequency was thereby selected as the excitation frequency of diagnostic signal in this parametric study.

Figure 5 shows the velocity (Fig. 5(a)) and magnitude (Fig. 5(b)) of  $S_0$  and  $A_0$  in the bone phantoms with soft phases of different thicknesses (0.8, 3.4, 4.2, 7.7 and 9.4 mm), highlighting observations that the coupled ASR layer exerts influence on both  $S_0$  and  $A_0$  obviously, exhibiting reductions in signal magnitudes and decreases in propagation velocities, for both whereas at different degrees. The most significant changes take place when the ASR layer is initially introduced, and decrease in signal magnitude continues as thickness of the ASR layer increases, but propagation velocities of both modes fluctuate very slightly with further increase of ASR thickness. It is different from

the case when a pure fluid layer serving as the soft phase (Section 4.1) in which prominent modulation on ultrasonic waves due to existence of coupled medium can be noticed for  $A_0$  only. To investigate the dependence of propagation velocities of two discussed wave modes on excitation frequency of the diagnostic signal,  $S_0$  and  $A_0$  were activated in a sweep frequency range from 50 to 200 kHz to propagate in the synthesised bone phantoms. The obtained dispersion curves of two modes in the absence and presence of a soft phase (a layer of ASR 3.4 mm in thickness) is plotted in Fig. 6. Results reiterate that the coupling effect of soft phase on  $S_0$  and  $A_0$  exists across the whole discussed frequency range: ASR exerts strong coupling influence on both wave modes, exhibiting as reduced propagation velocities.

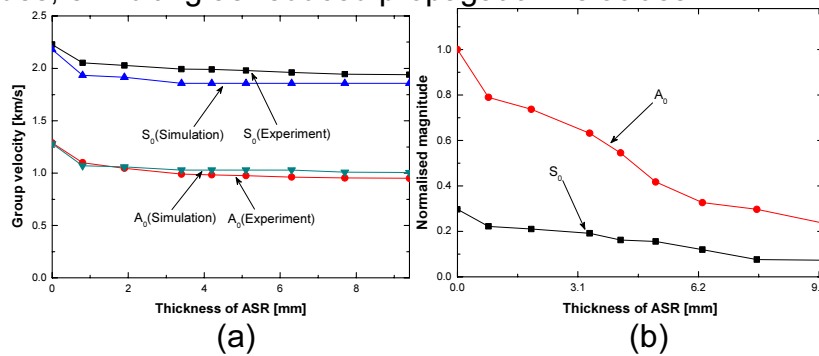


Fig. 5. **(a)** Group velocities and **(b)** magnitudes of  $S_0$  and  $A_0$  in bone phantoms (ASR thickness from 0.8 to 9.4 mm as mentioned before) vs. thickness of the coupled ASR layer (excitation frequency: 75 kHz; signal magnitude being normalised relative to the amplitude extremum of the signal in the absence of ASR)

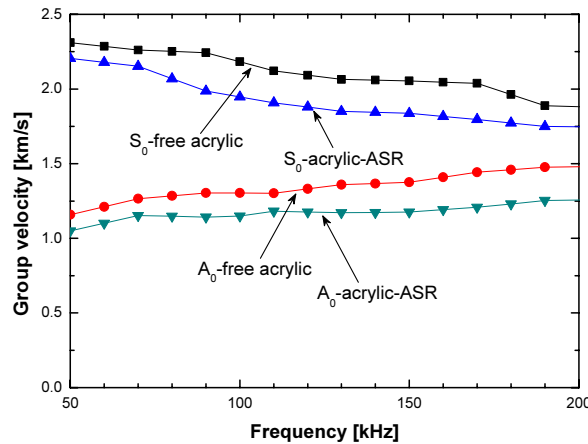


Fig. 6. Dispersion curves of  $S_0$  and  $A_0$  in bone phantoms without and with a layer of ASR (3.4 mm in thickness)

Throughout the study the most prominent modulations from a coupled soft phase on propagation velocities of  $S_0$  and  $A_0$  take place when the soft phase is initially introduced, and there is no phenomenal discrepancy in such a modulation when the soft phase has different thickness (Figs. 3 and 5(a)). This implies that the surrounding soft tissues exert perceptible influence on the speed of ultrasonic Lamb waves only in a

confined area, making it possible to extend the compensation for such an influence at a specific thickness of the soft phase to general cases, if only the propagation velocity is concerned in bone assessment. Nevertheless, a continuous and increasing modulation on signal magnitude can be seen with an increase in thickness (Fig. 5(b)) of ASR. It articulates that rectification for such a coupling effect is case-dependent and compensation should be applied according to the calibrated relationships between changes in signal magnitude and changes in soft phase (Fig. 5(b)) if signal magnitude is also a factor in bone assessment.

## 5. APPLICATIONS

### 5.1. Application to NDE for corrosion detection of submerged structures

In this section, the calibrated influence of fluid coupling on Lamb wave propagation (Section 4.1) was applied to the evaluation of a corrosion damage (15 mm in diameter and 1 mm in depth) in a submerged aluminium plate (600 mm × 600 mm × 1.6 mm) using the probability-based diagnostic imaging (Chen *et al.* 2010). A pair of water-proof immersion transducers, the same as that described in Section 3.2, was employed to perform a pulse-echo measurement at different positions at the interface of the fluid layer and aluminium plate, offering three sensing paths,  $T_1-R_1$ ,  $T_2-R_2$  and  $T_3-R_3$  (Fig. 7). Signal generation/acquisition was accomplished with the system developed on a VXI platform (Fig. 2).



Fig. 7. An aluminium plate containing corrosion damage

As is known, the presence of a layer of water significantly alters the propagation of Lamb waves in the plate, in particular the  $A_0$  (Figs. 3 and 4). If the coupling effect of water is not well considered and compensated, the final detection of the damage can be inaccurate. Such a concern was demonstrated in this section, as displayed in Fig. 8(a) (without compensation) and Fig. 8(b) (with compensation). It is clear that the detection precision has been significantly improved after compensation for the coupling effect.



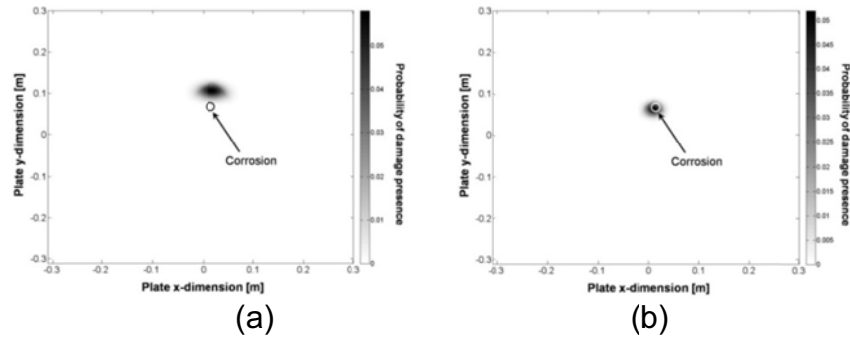


Fig. 8. Identification results of corrosion damage in the aluminium plate coupled with fluid layer of different thicknesses: **(a)** without rectification; and **(b)** with compensation for the coupling effect (the fluid layer is 4 mm in thickness) (white or black circle: actual corrosion)

### 5.2. Application to Monitoring of Mimicked Healing Progress of Fractured Bone

In clinical practice, diagnosis of osteoporosis or monitoring of healing progress of fractured bones (e.g. distal radius and hip) can be achieved with QUS techniques by detecting changes in the velocity of  $S_0$  or  $A_0$  with regard to baseline signals collected from healthy groups. When QUS is conducted *in vivo*, the coupling effect of soft tissues on  $S_0$  and  $A_0$  cannot be avoided, which is, however, sometimes neglected in the clinical practice, leading to compromised prediction accuracy [4]. In the following, as an application of the results arising from the above study, the coupling effect of soft tissues on  $A_0$  was compensated, so as to improve the accuracy of  $A_0$ -based QUS when used for predicting a certain healing status of mimicked bone fracture.

To simulate a fractured bone at different healing statuses, a series of samples was fabricated in accordance with the following procedures: two identical acrylic plates (230 mm  $\times$  240 mm  $\times$  3.2 mm each) were connected via an ASR strip (Young's modulus being 2.8 MPa), as sketched in Fig. 9(a). A total of seven such samples were made, each having an ASR strip of different width (along the axial direction of the sample), from 0 to 6 mm with an increment of 1 mm. These seven samples imitated a fractured bone at seven healing statuses (0 mm width standing for a healthy bone). A pair of transducers was placed atop these samples respectively in terms of the axial transmission technique as seen in Fig. 9(a). Five-cycle *Hanning*-window modulated sinusoidal tonebursts at 100 kHz were used as the diagnostic signal. Correlation between the reduction rate in the propagation velocity of  $A_0$  and width of callus was obtained, as shown in Fig. 10(a), which would be used to determine the healing progress of bone fracture. Note that the velocity of  $A_0$  shown in Fig. 10(a) was measured from the fractured bone sample without any coupled soft tissues (Fig. 9(a)).

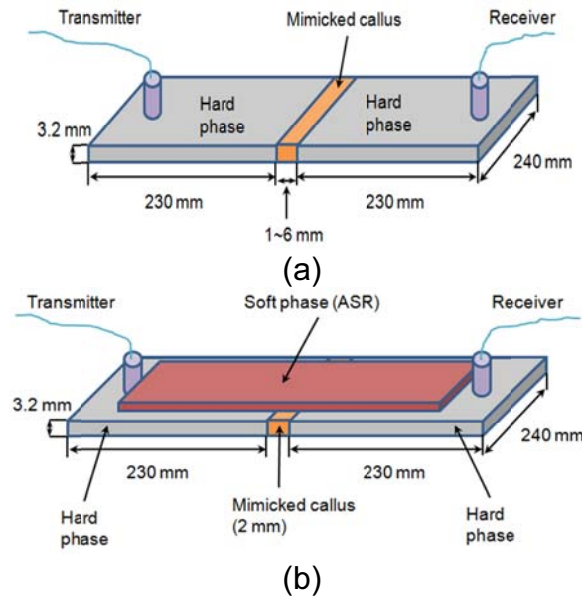


Fig. 9. Schematic of bone samples with mimicked callus for imitating bone fracture: **(a)** without coupled ASR layer; **(b)** with coupled ASR layer when callus is 2 mm wide

To introduce the coupling effect of soft tissues, a layer of ASR ( $160 \text{ mm} \times 60 \text{ mm} \times 3.4 \text{ mm}$ ,  $E_{ASR} = 11.96 \text{ kPa}$ ) was adhered to one of the above seven samples (with a callus width of 2 mm), serving as the overlying soft tissues, as elucidated in Fig. 9(b). As indicated in Fig. 10(b), there is a reduction of 23% in velocity of  $A_0$  in the specific bone fracture phantom comparing with that in the intact bone phantom. Referencing such a reduction to those in Fig. 10(a), the current bone fracture healing was determined to be 4 mm, which is, however, incorrect. This is because the reduction of 23% is not solely attributed to the callus, but the coupling effect of soft tissue. When the coupling effect was taken into account and compensated, the correct healing status can be obtained to be 2 mm.

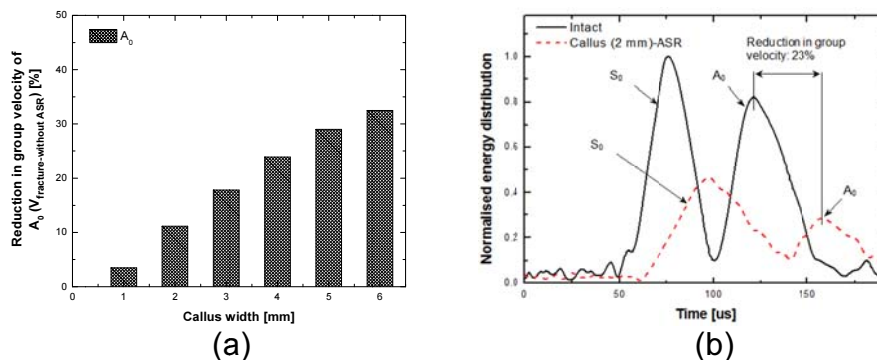


Fig. 10. **(a)** Reduction in propagation velocity of  $A_0$  vs. width of callus (reflecting different healing stages) (note: correlation in this figure was established in the absence

of overlying soft tissues); and **(b)** HT-processed results of signals experimentally captured from intact sample (containing neither callus nor coupled overlying soft tissues) and mimicked fractured bone sample (with both callus and coupled overlying soft tissues)

## 6. CONCLUSION

The effect of coupled medium (e.g., fluid or soft tissue) on Lamb wave propagation in engineering structures and human bones can pose great challenge on NDE and QUS techniques for delivering high precision evaluation. The investigation on such a coupling effect, conducted in this study, demonstrated that the  $S_0$  and  $A_0$  are sensitive to the coupling medium, manifested as reduced propagation velocity and signal magnitude as a result of the coupling. The alteration in the wave propagation resulted in impaired precision and accuracy of either NDE for corrosion in submerged structures or QUS for monitoring the healing progress of bone fracture. However, with consideration of and compensation for such a coupling effect, the precision and accuracy of both applications (NDE and QUS) were significantly improved, leading to precise prediction of the location of the corrosion and accurate determination of the current bone healing stage. This study recapitulates that coupling effect due to fluid/soft tissue on ultrasonic waves should be quantitatively taken into account when developing high-precision NDE and QUS techniques.

## REFERENCE

- Cheeke, J.D.N., Shannon, K. and Wang, Z. (1999), "Loading effects on A0 Lamb-like waves in full and partially filled thin-walled tubes", *Sens. Actuators, A*, **59**(2-3), 180-183.
- Chen, J., Su, Z. and Cheng, L. (2010), "Identification of corrosion damage in submerged structures using fundamental anti-symmetric Lamb waves", *Smart Mater. Struct.*, **19**(1), 015004.
- Moilanen, P., Nicholson, P.H.F., Kilappa, V., Cheng, S. and Timonen, J. (2006), "Measuring guided waves in long bones: Modeling and experiments in free and immersed plates", *Ultrasound. Med. Biol.*, **32**(5), 709-719.
- Na, W.B. and Kundu, T. (2002), "Underwater pipeline inspection using guided waves", *J. Press. Vess-T. ASME.*, **124**(2), 196-200.
- Palmeri, M.L., Sharma, A.C., Bouchard, R.R., Nightingale, R.W. and Nightingale, K.R. (2005), "A finite-element method model of soft tissue response to impulsive acoustic radiation force", *IEEE. T. Ultrason. Ferr.*, **52**(10), 1699-1712.
- Yapura, C.L. and Kinra, V.K. (1995), "Guided waves in a fluid-solid bilayer", *Wave Motion*, **21**(1), 35-46.